

# Cost Analysis for In-house versus Industry-printed Skull Models for Acute Midfacial Fractures

Lyfong S. Lor, BS\*  
 Dominic A. Massary, MD\*  
 Scotty A. Chung, MS†  
 Philip J. Brown, PhD†  
 Christopher M. Runyan, MD,  
 PhD\*

**Background:** Industry-printed (IP) 3-dimensional (3D) models are commonly used for secondary midfacial reconstructive cases but not for acute cases due to their high cost and long turnaround time. We have begun using in-house (IH) printed models for complex unilateral midface trauma. We hypothesized that IH models would decrease cost and turnaround time, compared with IP models.

**Methods:** We retrospectively examined cost and turnaround time data from midface trauma cases performed in 2017–2019 using 3D models (total, n = 15; IH, n = 10; IP, n = 5). Data for IH models were obtained through itemized cost reports from our Biomedical Engineering Department, where the models were printed. Data associated with IP models were obtained through itemized cost reports from our industry vendor. Perioperative data were collected from electronic medical records.

**Results:** The average cost for IH models ( $\$236.38 \pm 26.17$ ) was significantly less ( $P < 0.001$ ) than that for IP models ( $\$1677.82 \pm 488.43$ ). Minimal possible time from planning to model delivery was determined. IH models could be produced in as little as 4.65 hours, whereas the IP models required a minimum of 5 days (120 hours) from order placement. There were no significant differences in average operating room time ( $P = 0.34$ ), surgical complications, or subjective outcomes, but there was a significant difference in estimated blood loss ( $P = 0.04$ ).

**Conclusion:** Utilization of IH 3D skull models is a creative and practical adjunct to complex unilateral midfacial trauma that also reduces cost and turnaround time compared with IP 3D models. (*Plast Reconstr Surg Glob Open* 2020;8:e2831; doi: 10.1097/GOX.0000000000002831; Published online 26 May 2020.)

## INTRODUCTION

Since its invention in the 1980s, 3-dimensional (3D) printing technology, also known as additive manufacturing and rapid prototyping, has been an indispensable tool in manufacturing items, ranging from clothes and furniture to houses and aircrafts.<sup>1</sup> Technological advances

have expanded the utility of 3D printing to the realms of biology and medicine, as evidenced by a rapid increase in the number of publications in recent years involving medical applications of 3D printing.<sup>2,3</sup> This technology has been applied to numerous medical specialties, including orthopedics, neurosurgery, cardiac surgery, and plastic and reconstructive surgery. Several benefits of using 3D printed materials within medicine have been described in the literature. These include improved patient education and medical training, more effective preoperative planning, and improved surgical confidence, the net effect of which are better clinical outcomes with decreased intraoperative complications and operating room (OR) time.<sup>2,4-8</sup>

Craniofacial defects can result in functional limitations, such as the ability to properly speak, chew food, breathe, and see clearly. Defects in the craniofacial region are inherently difficult to treat because of the complex relationship of varied tissue types (bone, cartilage, muscle, and skin) and structures (auricle, orbit, nose, and oral cavity).<sup>5</sup> Furthermore, anatomical variances between patients necessitates patient-specific reconstructive approaches to optimize outcomes. To address this variability, 3D printing technology allows for production of patient-specific 3D

From the \*Department of Plastic and Reconstructive Surgery, Wake Forest Baptist Medical Center, Winston-Salem, N.C.; and †Biomedical Engineering, Virginia Tech-Wake Forest University School of Biomedical Engineering and Sciences, Winston-Salem, N.C. Received for publication December 18, 2019; accepted March 18, 2020.

Presented at the North Carolina Society of Plastic Surgeons and South Carolina Society of Plastic Surgeons Annual Meeting, November 3, 2018, Kiawah Island, S.C., and at the Wake Forest School of Medicine Medical Student Research Day, October 10, 2018, Winston-Salem, N.C.

Copyright © 2020 The Authors. Published by Wolters Kluwer Health, Inc. on behalf of The American Society of Plastic Surgeons. This is an open-access article distributed under the terms of the [Creative Commons Attribution-Non Commercial-No Derivatives License 4.0 \(CCBY-NC-ND\)](#), where it is permissible to download and share the work provided it is properly cited. The work cannot be changed in any way or used commercially without permission from the journal.

DOI: 10.1097/GOX.0000000000002831

**Disclosure:** The authors have no financial interest to declare in relation to the content of this article.

surgical models that can be used for precise contouring of hardware such as titanium plates to be used intraoperatively. In cases of unilateral facial trauma, many of these models are produced from a mirror image of the unaffected contralateral skull.<sup>9,10</sup> The use of 3D custom-printed models to guide reconstruction of facial defects is gaining popularity, particularly for secondary defects related to tumor extirpation and complex trauma.<sup>10-16</sup> In contrast, there is very little description of using contour models for treating acute traumatic midfacial fractures.<sup>9,17,18</sup>

Although benefits of craniofacial 3D models are apparent, high cost and long turnaround time prohibit an expanded use of industry-printed (IP) models.<sup>19,20</sup> In a study by Bosc et al,<sup>21</sup> 3D-printed cutting guides used for mandibular reconstruction cost between \$2497 and \$4993 per patient when using industry vendors. The average time to create cutting guides was 5.1 days and ranged from 3 to 15 days. A retrospective chart review done by Manrique et al<sup>22</sup> found that the mean cost of an implant for craniofacial reconstruction was  $\$8493 \pm \$837.95$  and the mean time required to manufacture the implants was 2 weeks. Such time requirements and costs limit the use of IP models in secondary reconstructive cases, rather than in acute trauma reconstruction. Bringing the 3D printing process in-house (IH) has the benefit of lowering cost and production time for reconstruction of secondary or delayed reconstructions. Numajiri et al<sup>23</sup> reported that 3D printing surgical guides for mandibular reconstruction could be produced for \$400. Others demonstrated that a mock patient-specific craniofacial reconstruction model could be produced for about \$250.<sup>24</sup> These studies have shown that costs and production time can be lowered for secondary or delayed reconstruction, but there is little information on applying this technology to treating acute craniofacial trauma.

To mitigate the high cost and long turnaround time of IP models, we have begun to partner with our Biomedical Engineering Department to design and print IH surgical models. We hypothesize that IH printed models will have significantly decreased associated costs and shorter turnaround time than the IP models. Our study seeks to compare the cost and outcomes of IH versus IP printed 3D surgical models while exploring the feasibility, benefits, and limitations of IH printing for acute craniofacial surgical reconstruction.

## METHODS

With IRB approval, we retrospectively collected data on all patients treated by the senior author from 2017 to 2019, with unilateral midfacial trauma for whom 3D-printed models were used. Patients undergoing secondary (delayed) reconstructive craniofacial procedures (n = 5) had IP models created, whereas IH-printed models were used for those patients treated for acute, zygomaticomaxillary complex fractures (n = 10). Perioperative and postoperative data of patients were collected from electronic medical records of patients. Patient's demographic data are shown in [Table 1](#).

IP models were provided by KLS Martin (Jacksonville, Fla.). Costs associated with these models were obtained through OR-generated itemized cost reports and through cost reports from KLS Martin. Costs associated with custom-implants or fixation materials were excluded from the analysis to isolate the costs of the models alone.

### IH Printing Process

Each patient underwent a preoperative axial spiral computed tomography (CT) scan with 0.625-mm slice thickness (Somatom Definition Flash; Siemens, Munich, Germany). 3D reconstructions of the scans were annotated by the senior surgeon (Fig. 1) to print a mirror image contralateral to the affected midface. A secure e-mail carrying instructions and relevant case details was then sent to the engineering team for preparation of the Digital Imaging and Communications in Medicine (DICOMs) and 3D printing.

Patients' DICOM files were imported into the segmentation software Mimics (Research v21.0 Materialise, Leuven, Belgium). Within Mimics, a gaussian filter was first applied on the images for noise reduction. Then a mask using the "Bone CT" threshold (226–3071 HU) was applied, which isolated the bony regions from other tissue, with further manual adjustments made of the threshold to remove artifacts. This mask was displayed as a 3D object and then exported as a standard tessellation (STL) file.

This STL file was then imported into the Geomagic Studio 2014 (3D Systems, Rock Hill, S.C.), a 3D object-editing software tool. A global quick smooth operation was performed to reduce artifactual irregularities on the surface of the model. The midline of the skull was determined by identifying regular midline bony landmarks (dental midlines, nasal base, center of sella, opisthocranion), and a midline plane was created. All points on the affected side of the plane were cropped, and the mandible and unaffected regions of the skull were also cropped. Using the same midline plane, a mirroring function was then applied to generate the reference model, which was exported as an STL file. Final conditioning of this STL file was performed using Netfabb Premium 2019 (Autodesk) for 3D printing, to correct any small errors that may occur from generating and modifying the STL file.

A Carbon M1 printer (Carbon Inc, Redwood, Calif.) with a 141 × 79 × 326-mm<sup>3</sup> workspace was used. The finalized STL file was uploaded to the Carbon 3D's web-based interface where the resin type, supports for the prints, and patient-specific labels were applied. All models were printed using urethane methacrylate (UMA 90; Carbon Inc, Redwood, Calif.). Postprocessing of the printed model includes the removal of uncured resin using isopropyl alcohol, additional ultraviolet curing, and minor sanding of support locations. The fabricated model was then delivered to the clinical team for preoperative planning.

The time was manually tracked and validated by reviewing the file details, which include the creation time stamp and last updated time stamp. The segmentation time category combined the time using Mimics, Geomagic, and Netfabb. Itemized cost reports for labor, printing time,

**Table 1. Demographics of Cases Using 3D Models**

Case	Age	Sex	Diagnosis	Mechanism of Injury	Other Craniofacial Surgery	Complications
1	3	M	L ZMC complex Fx, L orbital blowout Fx	Horse kick	None	None
2	37	M	Comminuted R ZMC Fx, R hemi Le Fort I Fx, R orbital floor blowout Fx	Assault	None	None
3	42	M	Frontal bone Fx, L naso-orbital ethmoid Fx type 2, L comminuted ZMC Fx, traumatic defect of one-third of L lower eyelid	GSW	Free ALT flap for coverage of submental wound, free flap debulking and debridement midface bone fragments, Removal of maxillary hardware and bony debridement	None
4	42	M	R ZMC Fx with orbital floor involvement	Assault	None	None
5	30	M	R subcondylar mandible Fx, L mandibular body Fx, L ZMC Fx, L hemi-Le Fort I Fx, nasal Fx.	MVC	None	None
6	33	M	R ZMC Fx, nasal Fx	MVC	None	None
7	47	M	R ZMC Fx	Fall	R frontotemporoparietal craniotomy for evacuation of acute epidural hematoma	None
8	40	M	L ZMC Fx	MVC	None	None
9	31	M	R ZMC Fx, L nondisplaced and non-mobile Le Fort I Fx, nasal Fx	MVC	None	None
10	7	F	R comminuted ZMC Fx, R maxillary wall comminuted Fx, R orbital blowout Fx, full-thickness L nasal ala defect	GSW	Irrigation and debridement of R ZMC open Fx × 2	None
11	59	M	Frontal scalp wound with exposed acrylic cranioplasty implant	Grade 3 astrocytoma s/p radiation and chemotherapy	Reconstruction of scalp wound with free latissimus dorsi myocutaneous flap and titanium mesh cranioplasty	None
12	23	F	L frontotemporoparietal skull defect	Failed bone flap	L frontotemporoparietal craniectomy, duraplasty	None
13	17	M	Cranial defect following gunshot wound to skull	GSW	PEEK cranioplasty	None
14	26	M	Electrical burn involving left facial skin, soft tissue, lateral orbital rim and upper zygomatic body	Burns	Reconstruction left facial defect with parascapular free flap and bone graft to lateral orbit, revision left lateral orbital reconstruction with PEEK implant, revision facial flap with lateral canthoplasty × 2	Partial resorption lateral orbit bone graft requiring alloplastic reconstruction, PEEK exposure, and ectropion
15	48	M	History of R orbital zygomatic Fx s/p ORIF, residual orbital zygomatic malposition, enophthalmos	MVC	Secondary orbitozygomatic reconstruction with split calvarial bone graft, Lateral canthopexy and gold weight placement	Eyelid ectropion and lagophthalmos

Cases 1–10 are in-house printed; cases 11–15 are industry-printed.

ALT, anterolateral thigh; Fx, fracture; GSW, gunshot wound; L, left; MVC, motor vehicle collision; ORIF, open reduction and internal fixation; PEEK, polyethyl-ethyl ketone; R, right; s/p, status post; ZMC, zygomaticomaxillary complex.

and material costs were generated and provided to the clinic team.

## RESULTS

Urgency of the surgical case was the most significant determining factor in turnaround time; if models were needed urgently, model production could be started immediately. We defined turnaround time as the minimum time required from order placement to receipt of the model. The statistical analysis throughout this study uses a paired sample *t* test. The minimum time necessary for receipt of an IP model was 120 hours (5 days). The minimum turnaround time for IH models ranged from 4.65 to 7.18 hours, with an average of  $5.7 \pm 0.64$  hours

and was significantly lower than the turnaround time of IP models ( $P < 0.001$ ).

IH model cost reports were itemized into the following 5 categories: software and disposable fees, segmentation labor, material cost, print time fees, and production labor (Table 2). Total costs for IH models varied based on time required for segmentation, printing, and post-production, as well as on the size of the model. The mean total cost was  $\$236.38 \pm 26.17$ .

Cost reports from our institution ORs and our vendor did not yield itemized cost breakdowns for direct comparison with our IH printed models. IP model costs ranged from \$708.33 to \$1995, with an average of  $\$1677.82 \pm 488.43$ . The increased cost for IP models was significant when compared with that for IH models ( $P < 0.001$ ).

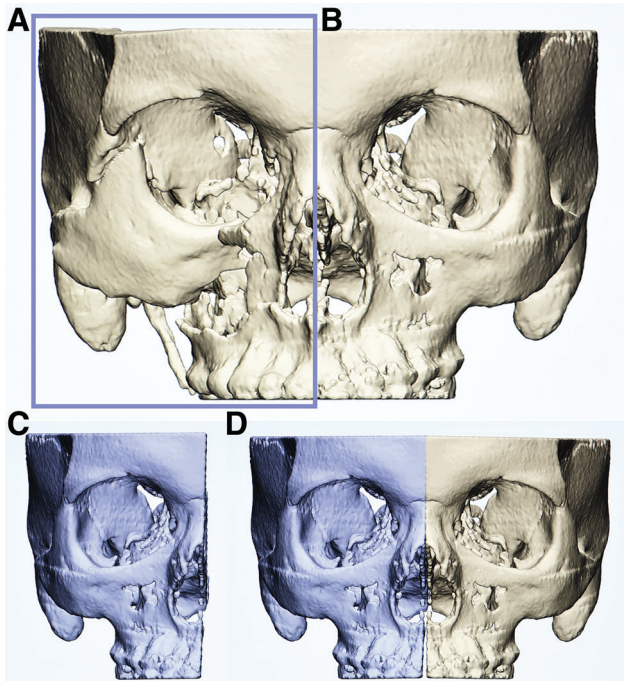


**Fig. 1.** Workflow for designing a mirrored, mid-face model. A, The unaffected hemi-midface region is identified and outlined. B, A mirror image of the unaffected hemi-midface is created using Materialise Mimics software. This will then be 3D-printed for use as an intraoperative guide for prebending fixation hardware. C, This graphic demonstrates the combined unaffected hemi-skull and mirror imaged hemi-midface (blue) to simulate the reconstructive goal.

**Table 2. IH Model Cost Report**

In-house Cost Breakdown Categories	Price per Unit (USD)	Total Average Price per Category per Model (USD)
Software and disposable fees	30–45	34.5 ± 4.90
Segmentation labor	30/h	43.80 ± 14.19
Material cost	0.14/mL	11 ± 1.76
Print time fees	32/h	65.60–117.87
Production labor	20/h	20.50 ± 2.71
Total		236.38 ± 26.17

USD, US dollars.

Total OR time was defined as the time from the incision to procedure completion. OR time for cases using IH models ranged from 107 to 344 minutes and averaged  $186.2 \pm 56.86$  minutes, while cases using IP models ranged from 113 to 272 minutes with an average of  $239.2 \pm 129.14$  minutes ( $P = 0.34$ ). Estimated blood loss in cases using IH printed models ranged from 20 to 250 mL, averaging  $63 \pm 56.8$  mL, which was lower than the blood loss for cases using IP models (range of 100–200 mL; mean of  $170 \pm 82$  mL;  $P = 0.04$ ). No revisionary operations were required to improve bony reduction or fixation in either group. [Figure 2](#) demonstrates a typical clinic case.

## DISCUSSION

To the author’s knowledge, this study is the first to analyze cost and time savings associated with using IH 3D

models compared with IP 3D models for acute midfacial trauma. Using mirror image skull models is a creative and practical adjunct to complex and debilitating midfacial trauma. These models allow for a more efficient and precise contouring of hardware such as titanium plates to be used intraoperatively, decreasing surgical complications and increasing surgeon confidence. Manufacturing these models IH significantly reduces the cost and turnaround time compared with IP models, without affecting operative time or subjective outcomes. However, there was a significant difference in estimated blood loss. This difference was not surprising and was consistent with the different nature of secondary delayed reconstructive procedures versus primary acute reconstruction. We expected secondary reconstructions to have longer operative times and therefore greater blood loss. Our data support the longer average operative times that we expected to see with secondary reconstruction, though this difference was not statistically significant.

The transfer of the patient’s CT scan from the clinical team to the printing team saves time and is greatly simplified by not having to go out of the medical center’s network. Additionally, the direct communication between the clinical and printing team removes any delay if questions arise. Due to the close proximity of the Wake Forest Biomedical Engineering department and our hospital, models can be delivered and used immediately upon completion of model manufacturing, further decreasing turnaround time. The significant reduction in turnaround time allows for the use of patient-specific models for acute facial trauma, with next-day turnaround time.

Despite the advantages to using 3D models in acute midfacial reconstruction, this technology may not be generally applicable. Our study limited the use of these models to cases with unilateral facial trauma due to the necessity of an unaffected side from which we could make a mirror image 3D print. Patients with bilateral facial trauma or inherent facial asymmetry may not have the symmetry necessary for the accurate utilization of these models. In the hands of experienced craniofacial surgeons, the use of models for contouring plates is not typically necessary for non- or minimally displaced fractures. We feel the approach is best suited for cases of severe facial trauma, including those with significant displacement, comminution, or those requiring bone grafting. Additionally, not every institution may be able to produce IH models due to the high startup cost of the necessary equipment and/or lack of available biomedical collaborators. Finally, we do not have objective outcome measures on the accuracy of the facial reduction compared with cases where models were not used.

This study is not without limitations. One such limitation is the relatively small and unequal sample sizes of the cohorts corresponding to IH ( $n = 10$ ) versus IP ( $n = 5$ ) models, potentially decreasing the power of our study. There was also a lack of standard defect severity between cases and cohorts. Larger and more complex deformities would have had greater associated costs, and it is plausible that this lack of standard defect severity may influence the overall results of this cost analysis. Additionally, we

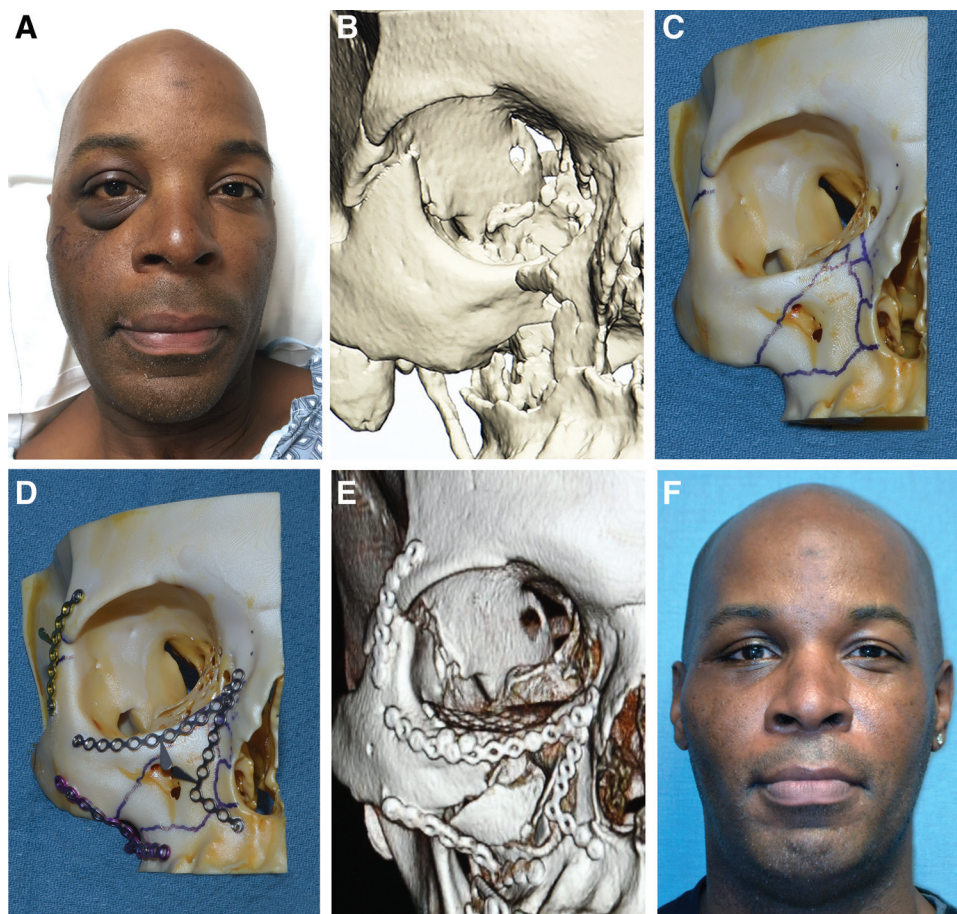


**Fig. 2.** Application of the IH-printed model for repair of a unilateral midfacial fracture. This patient was assaulted, sustaining a right zygomaticomaxillary complex and hemi-Lefort 1 fracture. A, He presented with significantly decreased malar projection, malocclusion, and on CT scan (B) with medial impaction of the zygoma and comminution of the midface. C, An IH-printed 3D model mirrored off of the contralateral side was marked on the operative field for locations of fracture lines, based on the CT scan. D, Midface titanium plates were selected to span key fracture segments and pre-bent and fixated to the model. E Postoperative CT demonstrates concordance of the predicted reduction and plate location, with the model. F, At 6 weeks following surgery, improvement in malar projection and facial width is noted.

are aware that in some instances, custom 3D-printed pre-bent plate implants are generated to precisely match the planned reconstruction. However, these custom 3D plate implants are very expensive. We are also of the opinion that it is not realistic for individual institutions to produce their own custom 3D plate implants due to hurdles such as Food and Drug Administration regulations regarding implantable materials. We believe that rather, using custom 3D skull models to then contour standard, malleable implantable plates reduces overall cost. The potential cost savings associated with producing custom 3D skull models instead of custom implantable hardware were not analyzed as part of this study. Finally, we did not compare the accuracy of our IH models to IP models. Our group is actively doing research in this area using a regional deviation analysis and we hope to share those findings in a future manuscript. However, our IH models are of high quality and are indistinguishable from IP models. Thus, we do not expect to see a dramatic difference in accuracy.

The American Medical Association has now approved the use of new CPT codes, which may be used for seeking reimbursement for individually prepared 3D-printed models (0559T, 0560T) and cutting guides (0561T, 0562T). As insurance companies evaluate reimbursement for these codes, cost analyses such as those conducted in this study may be useful in assessing minimal costs necessary for patient-specific stereolithographic models. Such models have been demonstrated to result in improved fracture reduction and patient outcomes for orbital and mandibular fractures.<sup>9,10,12-14,25,26</sup> Further studies are warranted to investigate the quality of fracture reduction and patient outcomes for those with complex facial trauma.

*Christopher M. Runyan, MD, PhD*

Department of Plastic and Reconstructive Surgery  
Wake Forest Baptist Medical Center  
1 Medical Center Blvd  
Winston-Salem, NC 27157  
E-mail: [crunyan@wakehealth.edu](mailto:crunyan@wakehealth.edu)

### PATIENT CONSENT STATEMENT

The patient provided written consent for the use of his image.

### REFERENCES

- Bauermeister AJ, Zuriarrain A, Newman MI. Three-dimensional printing in plastic and reconstructive surgery: a systematic review. *Ann Plast Surg.* 2016;77:569–576.
- Tack P, Victor J, Gemmel P, et al. 3D-printing techniques in a medical setting: a systematic literature review. *Biomed Eng Online.* 2016;15:115.
- Crafts TD, Ellsperman SE, Wannemuehler TJ, et al. Three-dimensional printing and its applications in otorhinolaryngology–head and neck surgery. *Otolaryngol Head Neck Surg.* 2017;156:999–1010.
- Gross BC, Erkal JL, Lockwood SY, et al. Evaluation of 3D printing and its potential impact on biotechnology and the chemical sciences. *Anal Chem.* 2014;86:3240–3253.
- Nyberg EL, Farris AL, Hung BP, et al. 3D-printing technologies for craniofacial rehabilitation, reconstruction, and regeneration. *Ann Biomed Eng.* 2017;45:45–57.
- Jacobs CA, Lin AY. A new classification of three-dimensional printing technologies: systematic review of three-dimensional printing for patient-specific craniomaxillofacial surgery. *Plast Reconstr Surg.* 2017;139:1211–1220.
- Nicot R, Druelle C, Schlund M, et al. Use of 3D printed models in student education of craniofacial traumas. *Dent Traumatol.* 2019;35:296–299.
- D'Souza N, Mainprize J, Edwards G, et al. Teaching facial fracture repair: a novel method of surgical skills training using three-dimensional biomodels. *Can J Plast Surg.* 2015;23:81–86.
- Xue R, Lai Q, Sun S, et al. Application of three-dimensional printing technology for improved orbital-maxillary-zygomatic reconstruction. *J Craniofac Surg.* 2019;30:e127–e131.
- Cohen A, Laviv A, Berman P, et al. Mandibular reconstruction using stereolithographic 3-dimensional printing modeling technology. *Oral Surg Oral Med Oral Pathol Oral Radiol Endod.* 2009;108:661–666.
- Eppley BL. Craniofacial reconstruction with computer-generated HTR patient-matched implants: use in primary bony tumor excision. *J Craniofac Surg.* 2002;13:650–657.
- Azuma M, Yanagawa T, Ishibashi-Kanno N, et al. Mandibular reconstruction using plates prebent to fit rapid prototyping 3-dimensional printing models ameliorates contour deformity. *Head Face Med.* 2014;10:45.
- Salgueiro MI, Stevens MR. Experience with the use of pre-bent plates for the reconstruction of mandibular defects. *Craniofacial Trauma Reconstr.* 2010;3:201–208.
- Podolsky DJ, Mainprize JG, Edwards GP, et al. Patient-specific orbital implants: development and implementation of technology for more accurate orbital reconstruction. *J Craniofac Surg.* 2016;27:131–133.
- Callahan AB, Campbell AA, Petris C, et al. Low-cost 3D printing orbital implant templates in secondary orbital reconstructions. *Ophthalmic Plast Reconstr Surg.* 2017;33:376–380.
- Kozakiewicz M, Szymor P. Comparison of pre-bent titanium mesh versus polyethylene implants in patient specific orbital reconstructions. *Head Face Med.* 2013;9:32.
- Cui J, Chen L, Guan X, et al. Surgical planning, three-dimensional model surgery and preshaped implants in treatment of bilateral craniomaxillofacial post-traumatic deformities. *J Oral Maxillofac Surg.* 2014;72:1138.e1–1138.e14.
- Feng F, Wang H, Guan X, et al. Mirror imaging and preshaped titanium plates in the treatment of unilateral malar and zygomatic arch fractures. *Oral Surg Oral Med Oral Pathol Oral Radiol Endod.* 2011;112:188–194.
- Gerstle TL, Ibrahim AM, Kim PS, et al. A plastic surgery application in evolution: three-dimensional printing. *Plast Reconstr Surg.* 2014;133:446–451.
- Hsieh TY, Dedhia R, Cervenka B, et al. 3D printing: current use in facial plastic and reconstructive surgery. *Curr Opin Otolaryngol Head Neck Surg.* 2017;25:291–299.
- Bosc R, Hersant B, Carloni R, et al. Mandibular reconstruction after cancer: an in-house approach to manufacturing cutting guides. *Int J Oral Maxillofac Surg.* 2017;46:24–31.
- Manrique OJ, Lalezarzadeh F, Dayan E, et al. Craniofacial reconstruction using patient-specific implants polyether ether ketone with computer-assisted planning. *J Craniofac Surg.* 2015;26:663–666.
- Numajiri T, Nakamura H, Sowa Y, et al. Low-cost design and manufacturing of surgical guides for mandibular reconstruction using a fibula. *Plast Reconstr Surg Glob Open.* 2016;4:e805.
- Msallem B, Beiglboeck F, Honigmann P, et al. Craniofacial reconstruction by a cost-efficient template-based process using 3D printing. *Plast Reconstr Surg Glob Open.* 2017;5:e1582.
- Park SW, Choi JW, Koh KS, et al. Mirror-imaged rapid prototype skull model and pre-molded synthetic scaffold to achieve optimal orbital cavity reconstruction. *J Oral Maxillofac Surg.* 2015;73:1540–1553.
- Mustafa SF, Evans PL, Bocca A, et al. Customized titanium reconstruction of post-traumatic orbital wall defects: a review of 22 cases. *Int J Oral Maxillofac Surg.* 2011;40:1357–1362.